

Physiological consequences of loss of plasminogen activator gene function in mice

Peter Carmeliet^{*†‡}, Luc Schoonjans[†], Lena Kieckens^{†‡}, Beverly Ream^{*}, Jay Degen[§], Roderick Bronson^{||}, Rita De Vos[¶], Joost J. van den Oord[¶], Désiré Collen^{†#} & Richard C. Mulligan^{*#}

* Whitehead Institute of Biomedical Research and the Department of Biology, Massachusetts Institute of Technology, Cambridge, Massachusetts 02142, USA

† Center for Molecular and Vascular Biology, University of Leuven, B-3000 Leuven, Belgium

§ Children's Hospital Research Foundation, University of Cincinnati, Ohio 45229-3039, USA

|| School of Veterinary Medicine, Tufts University, Boston, Massachusetts 01536, USA

¶ Laboratory of Histo- and Cytochemistry, University of Leuven, B-3000 Leuven, Belgium

Indirect evidence suggests a crucial role for the fibrinolytic system and its physiological triggers, tissue-type (t-PA) and urokinase-type (u-PA) plasminogen activator, in many proteolytic processes. Inactivation of the t-PA gene impairs clot lysis and inactivation of the u-PA gene results in occasional fibrin deposition. Mice with combined t-PA and u-PA deficiency suffer extensive spontaneous fibrin deposition, with its associated effects on growth, fertility and survival.

MAMMALIAN blood contains an enzymatic system, called the fibrinolytic system or the plasminogen/plasmin system, which has been claimed to play a role in a variety of phenomena associated with proteolysis, including blood clot dissolution (thrombolysis), ovulation, embryo implantation, embryogenesis, cell invasion and brain function¹⁻³. The fibrinolytic system comprises an inactive proenzyme, plasminogen, which is activated to the proteolytic enzyme plasmin by two physiological plasminogen activators, tissue-type plasminogen activator (t-PA) and urokinase-type plasminogen activator (u-PA). These are products of two separate genes with different genomic organization and chromosome localization².

t-PA is believed to be primarily responsible for removal of fibrin from the vascular tree²; it has a specific affinity for fibrin and produces clot-restricted plasminogen activation. The role of u-PA in thrombolysis is less well defined; it lacks affinity for fibrin and requires conversion from an inactive single-chain precursor to a catalytically active two-chain derivative². Whether other plasminogen activation pathways, such as the 'intrinsic' pathway (involving blood coagulation factor XII, high-molecular-mass kininogen, prekallikrein, and possibly u-PA⁴) contribute to clot lysis, remains to be established.

Urokinase-type plasminogen activator binds to a specific cell-surface receptor⁵ and is believed to be primarily involved in cell-mediated proteolysis by activation of latent matrix-degrading proteinases or growth factors^{6,7}. Its localization on the migrating front of cells suggests involvement in cell invasion through extracellular matrices^{3,6}. Directional proteolysis could play a role in physiological processes such as macrophage invasion⁸⁻¹⁰, ovulation^{11,12}, angiogenesis^{7,13} and wound healing^{7,14}, and in pathological cell invasion in neoplasia and metastasis¹⁵.

Fibrinolysis has been claimed to be involved in ovulation, fertilization, embryo implantation and embryogenesis, on the basis of its expression in ovulating oocytes^{8,10}, in migrating sperm cells¹⁶, in invading trophoblasts¹⁷ and in several primitive organs during embryogenesis^{18,19}. In addition, serine-proteinase

inhibitors and/or plasminogen-activator-specific antisera suppress ovulation¹² and embryo implantation²⁰.

The fibrinolytic system may also contribute to several pathological processes such as thrombosis²¹, atherosclerosis²², glomerulonephritis²³, acute respiratory distress syndrome²⁴, haemangioma formation¹³ and metastasis¹⁵. To date, genetic deficiencies of t-PA or u-PA have not been reported in man. Consequently, the implied role of the fibrinolytic system *in vivo* is deduced from correlations between fibrinolytic activity and (patho)physiological phenomena, which does not allow a causative role of the fibrinolytic system in these disorders to be established.

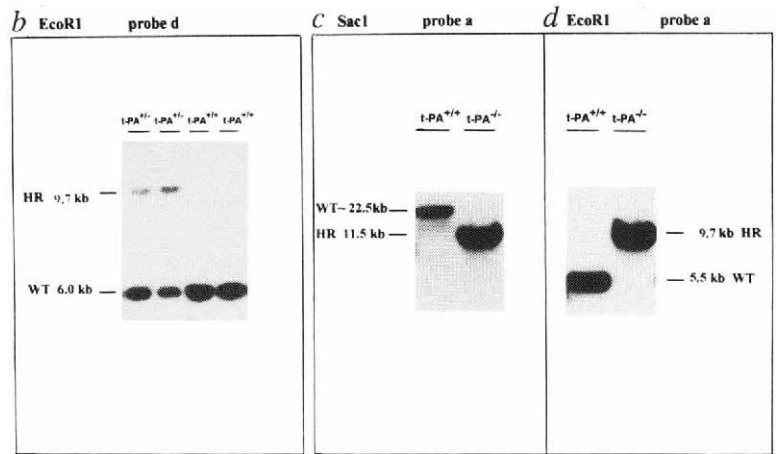
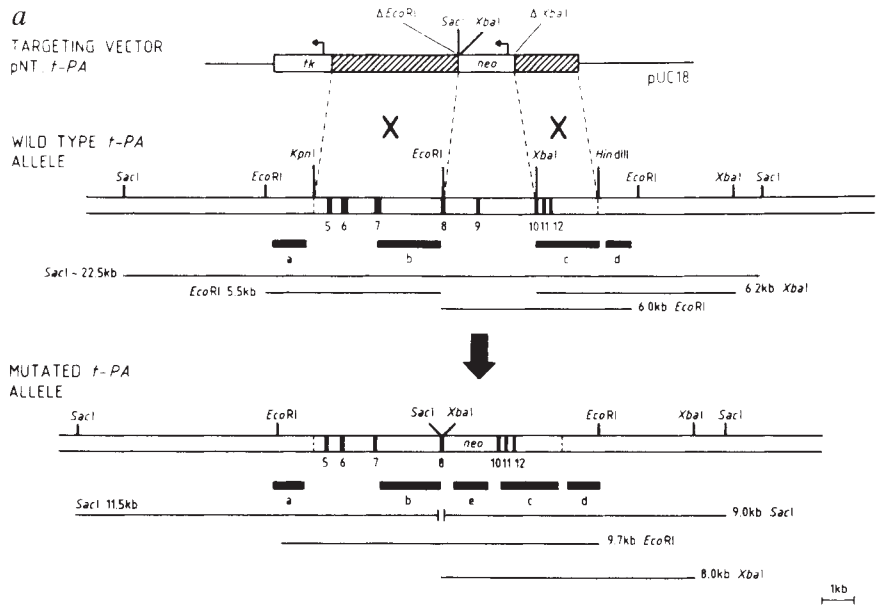
To investigate the role of t-PA- and u-PA-mediated plasminogen activation in development, reproduction, thrombolysis, thrombosis and macrophage function, we have generated mice with single and combined inactivation of the t-PA and/or u-PA genes. Mice with single deficiencies of t-PA or u-PA develop normally, are fertile and have a normal life span. t-PA-deficient mice had a reduced thrombolytic potential and increased incidence of endotoxin-induced thrombosis. u-PA-deficient mice occasionally developed spontaneous fibrin deposits in normal and inflamed tissues, revealed a higher incidence of endotoxin-induced thrombosis and displayed deficient plasmin-mediated macrophage function. Mice with combined deficiency of t-PA and u-PA survived embryonic development but suffered retarded postnatal growth, markedly reduced fertility and shortened life span. Furthermore, spontaneous fibrin deposition occurred more extensively, at an earlier age and in more organs than in mice with single u-PA deficiency.

Targeting of the t-PA and u-PA genes

To disrupt the t-PA gene, the targeting vector pNT.t-PA was constructed in which a cassette expressing the neomycin-resistance gene (*neo*) replaced the genomic sequences encoding most of the kringle-2 domain and part of the proteinase domain, including the catalytically essential histidine residue at position 326 (Fig. 1a). In the targeting vector used to disrupt the u-PA gene, pNT.u-PA, *neo* replaced the genomic sequences encompassing all but 23 amino acids of the coding sequence (Fig. 2a). Thus, the correct homologous recombination resulted in total

† Present address: Center for Molecular and Vascular Biology, University of Leuven, Campus Gasthuisberg, Herestraat 49, B-3000 Leuven, Belgium.
To whom correspondence should be addressed.

FIG. 1 Outline of the strategy used to disrupt the t-PA gene, and Southern blot analysis of genomic DNA. a, Schematic representation of the targeting vector pNT.t-PA used for disruption of the t-PA gene, of the wild-type t-PA allele and of the homologously recombined t-PA allele. pNT.3't-PA was generated by cloning a 2.0-kilobase (kb) 3'-flanking XbaI-HindIII fragment of the murine t-PA gene (isolated from a D₃ ES cell genomic DNA library provided by R. Jaenisch) into the XbaI site of the parental vector pNT by blunt-end ligation³⁴. pNT.t-PA was constructed by blunt-end ligation of a 4.3 kb 5'-flanking KpnI-EcoRI fragment of the murine t-PA gene into the EcoRI site of pNT.3't-PA. The EcoRI site of the 5'-flanking KpnI-EcoRI fragment is at base pair (bp) 810 and the XbaI site of the 3'-flanking XbaI-HindIII fragment is at bp 1,170 of the murine t-PA cDNA (notation as in ref. 35). The downstream EcoRI site in the 5'-flanking fragment and the upstream XbaI site in the 3'-flanking fragments were destroyed during the cloning process as denoted by ΔEcoRI and ΔXbaI. The targeting vector, wild-type and mutated allele are represented by double lines; shaded boxes denote 5'- and 3'-flanking regions of the targeting vector; filled boxes denote exons. Relative sizes of introns are approximate and based on mapping information of the rat t-PA gene³⁶. Only exons that were mapped by Southern blot analysis are shown and numbered. The expected restriction fragments of the wild-type and the targeted mutated allele are indicated with their relative sizes by underlining. Black boxes under the genomic structure denote the probes used for Southern blot analysis. Probe 'a' is a 0.5 kb EcoRI-XbaI genomic DNA fragment, located adjacent at the 5' site of the flanking regions of pNT.t-PA. Probe 'b' is a 2.2-kb XbaI-EcoRI genomic DNA fragment and probe 'c' a 2.0-kb XbaI-HindIII genomic DNA fragment, contained in the 5' or 3' flanking regions, respectively. Probe 'd' encompasses a 1.0-kb HindIII-EcoRI genomic fragment adjacent to the 3' XbaI-HindIII fragment used for the targeting construct. Probe 'e' is a 600-bp PstI fragment from the neo gene. b, Southern blot analysis of genomic DNA from D₃ embryonic stem cells, digested with EcoRI and hybridized to the 3' t-PA flanking probe 'd', showing two t-PA^{+/+} ES cell colonies, harbouring a 6.0-kb EcoRI fragment of the wild-type allele and a 9.7-kb EcoRI fragment of the mutated t-PA allele. t-PA^{+/+} ES cell clones were identified in 10% of all double-resistant ES cell clones, electroporated with pNT.t-PA. c, d, Southern blot analysis of genomic tail-tip DNA of t-PA^{+/+}



inactivation of the t-PA and u-PA genes, respectively. Site-specific and single homologous recombination at the t-PA and u-PA locus, respectively, were verified by Southern blot analysis of genomic DNA, using external and internal t-PA or u-PA probes, respectively, and a neo-specific probe (Figs 1 and 2).

Generation of mice with deficiencies

Mice with a single deficiency of t-PA or u-PA were generated by blastocyst injection of embryonic stem cell clones, harbouring a homologously recombined t-PA allele (heterozygous t-PA-deficient cells, t-PA^{+/-}; Fig. 1b) or u-PA allele (heterozygous u-PA-deficient cells, u-PA^{+/-}; Fig. 2b), respectively. Genotyping of 1,610 progeny from t-PA^{+/-} and of 703 offspring from u-PA^{+/-} breeding pairs by Southern blot analysis of tail DNA, obtained at three weeks of age (Figs 1c, d and 2c, d), revealed independent autosomal mendelian inheritance of the mutated t-PA and u-PA alleles. No differences in the litter size, the frequency of litters, the body weight of mice at 5 weeks of age or in the lifespan were found between t-PA wild-type (t-PA^{+/+})

and t-PA^{-/-} littermates, digested with SacI and EcoRI, and hybridized to probe 'a'. The observed sizes of the restriction fragments correspond to those expected for homologous recombination of the targeting vector pNT.t-PA into the t-PA locus.

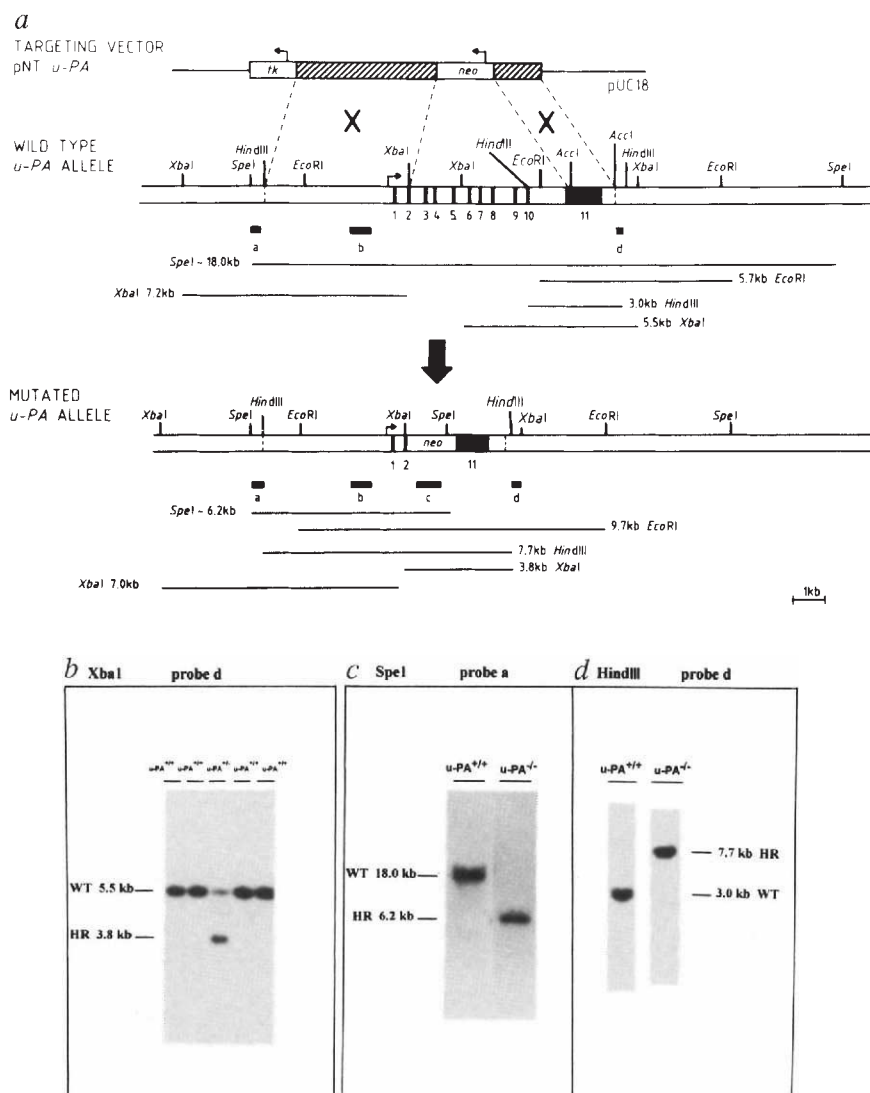
METHODS. Culture, transfection and selection of embryonic stem cells, and isolation, restriction digestion and Southern blot analysis of genomic DNA were as previously described³⁷.

and homozygous t-PA-deficient (t-PA^{-/-}) mice and between u-PA wild-type (u-PA^{+/+}) and homozygous u-PA-deficient (u-PA^{-/-}) mice (see supplementary information).

Correct targeting of the t-PA and u-PA genes was confirmed by the absence of detectable t-PA-specific or u-PA-specific messenger RNA and immunoreactivity (see supplementary information) and functional activity (Table 1). The t-PA activity in lung extracts and u-PA activity in kidney extracts and urine correlated closely with the numbers of functional t-PA or u-PA alleles, respectively. A compensatory increase of t-PA activity in brain extracts from u-PA^{-/-} mice or of u-PA activity in 24-h urine samples from t-PA^{-/-} mice could not be documented.

To examine the effect of a combined deficiency of t-PA and u-PA on viability, genotypes of 489 progeny from double heterozygous breeding pairs (t-PA^{+/-}:u-PA^{+/-}) were determined by Southern blot analysis at 3 weeks of age. Independent autosomal mendelian inheritance of the mutated t-PA and u-PA alleles was observed (see supplementary information). Compared to wild-type mice or mice with single deficiencies, mice with combined

FIG. 2 Outline of the strategy to disrupt the u-PA gene, and Southern blot analysis of genomic DNA. **a**, Schematic representation of the targeting vector pNT.u-PA used for disruption of the u-PA gene, of the wild-type u-PA allele and of the homologously recombined u-PA allele. pNT.u-PA was generated by cloning a 4.3-kb fragment from plasmid pBSMuPAneo[8.60RiB]tk (provided by J. Degen), containing the 5'-flanking *HindIII*-*XbaI* genomic fragment, into the *XbaI* site of pNT. The *XbaI* site in the 5'-flanking fragment is at bp +398 of the murine u-PA gene, 22 bp upstream of the ATG start codon (notation as in ref. 38). A 1.3-kb 3'-flanking *AccI* genomic fragment (isolated from the D₃ ES cell genomic DNA library, provided by R. Jaenisch) was then cloned into the *XhoI* site of pNT.u-PA by blunt end ligation to form pNT.u-PA. The upstream *AccI* in the 3'-flanking fragment is at bp +5,711 of the murine u-PA gene, 72 bp upstream of TGA stop codon³⁸. The resulting targeted u-PA allele contains exon 1 and 14 bp of exon 2 (non-coding sequence) and 999 bp of exon 11 (including 23 amino acids of coding sequence). Notation is as in Fig. 1a. Probe 'a' is a 0.20-kb *SpeI*-*HindIII* genomic fragment, adjacent 5' to the *HindIII*-*XbaI* flanking region; probe 'b' is a 0.64-kb *PvuII* genomic fragment contained in the 5'-flanking fragment (bp -963 to -320 of the murine u-PA gene)³⁸; probe 'c' is a 0.60-kb *PstI* fragment from the *neo* gene; probe 'd' is a 0.24-kb *AccI*-*HindIII* genomic fragment (bp +7,040 to +7,280 of the murine u-PA gene)³⁸, adjacent 3' to the *AccI* flanking fragment. **b**, Southern blot analysis of genomic DNA from D₃ embryonic stem cells, digested with *XbaI* and hybridized to the 3' u-PA flanking probe 'd', revealing an ES cell colony, harbouring a 5.5-kb *XbaI* fragment of the wild-type allele and a 3.8-kb *XbaI* fragment of the mutated u-PA allele. u-PA^{+/-} ES cell clones were identified in 2.5% of all double resistant ES cell clones, electroporated with pNT.u-PA. **c, d**, Southern blot analysis of genomic tail-tip DNA of u-PA^{+/+} and u-PA^{-/-} littermates, digested with *SpeI* and *HindIII*, and hybridized to probe 'a' and 'd', respectively. The observed sizes of the restriction fragments correspond to those expected for homologous recombination of the targeting vector pNT.u-PA into the u-PA locus.



homozygous deficiency of t-PA and u-PA (t-PA^{-/-}:u-PA^{-/-}) had a shorter lifespan (9 of 22 t-PA^{-/-}:u-PA^{-/-} mice but all of 15 wild-type mice survived until the end of an observation period of 30 to 40 weeks, whereas 3 of 10 double-deficient and all of 25 wild-type mice survived for 40 to 50 weeks; $P < 0.001$, by chi-square analysis). Double-deficient mice suffered growth retardation beyond the age of 3 weeks (body weights were 22 ± 1.5 g, $n = 14$, for t-PA^{-/-}:u-PA^{-/-} mice versus 33 ± 2.2 g, $n = 11$, for t-PA^{+/+}:u-PA^{+/+} mice at 23 weeks, $P < 0.0001$). They were also significantly less fertile: of the 19 double-deficient breeding pairs that were test-bred for at least 10 weeks, 6 did not produce any litter, 4 produced 1 litter, 7 produced 2 litters and 2 produced 3 litters. In contrast, 6 of 9 wild-type breeding pairs produced 2 litters and 3 of 9 wild-type breeding pairs produced 3 litters during similar breeding periods (see supplementary information). t-PA^{-/-}:u-PA^{-/-} breeding pairs produced slightly fewer offspring per litter than t-PA^{+/+}:u-PA^{+/+} breeding pairs: 4.8 ± 0.4 ($n = 30$) versus 6.2 ± 0.3 mice per litter ($n = 53$; $P = 0.007$).

Macroscopic and microscopic analysis

No macroscopic abnormalities were observed in t-PA^{-/-} mice up to an age of 14 months. u-PA^{-/-} mice developed rectal pro-

METHODS. Culture, transfection and selection of embryonic stem cells, and isolation, restriction digestion and Southern blot analysis of genomic DNA were as previously described³⁸.

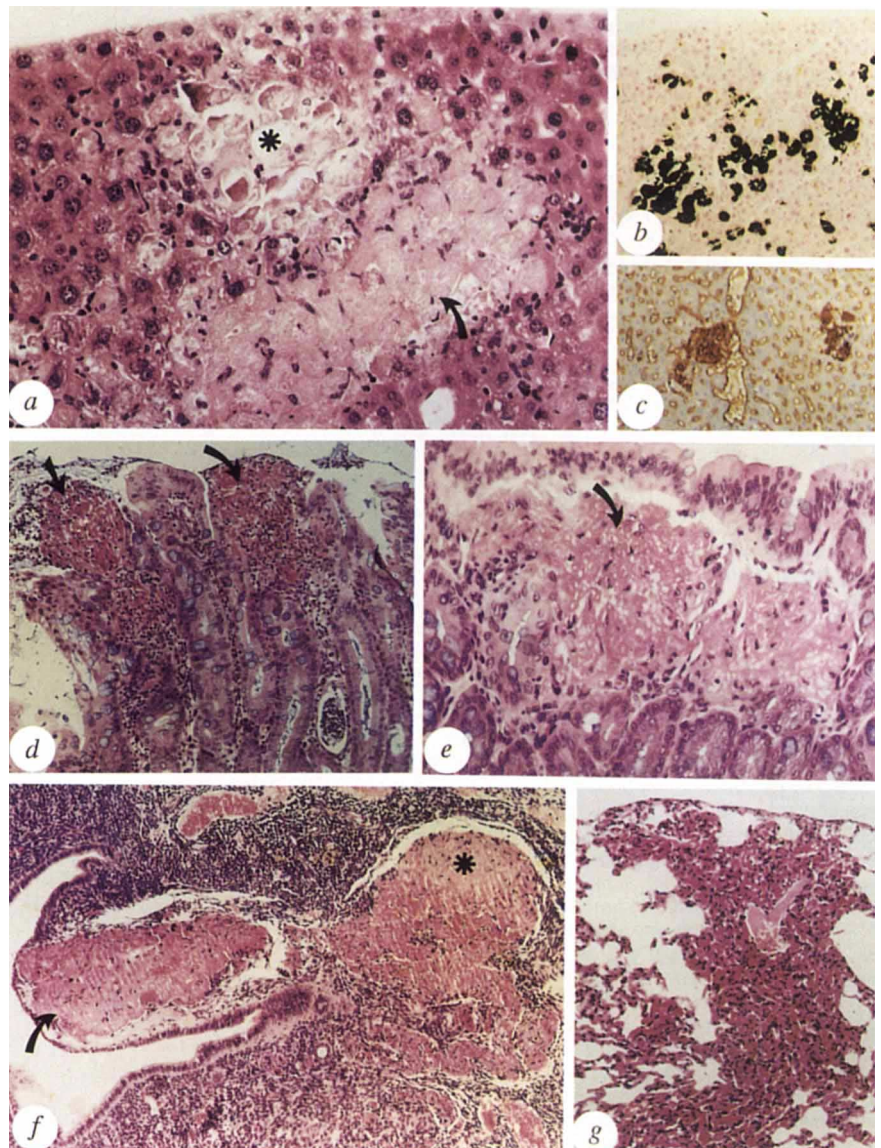
lapse of a non-infectious origin (6 out of 281 mice of 22 ± 0.8 weeks of age; 9%) and/or suffered extensive non-healing ulcerations at the eyelids, the ears around the eartag and the face, possibly resulting from the tagging trauma or scratching against the cage grid during feeding (12 of 281 mice of 26 ± 4 weeks of age; 5%).

From the age of 8 to 12 weeks on, t-PA^{-/-}:u-PA^{-/-} mice developed the following pathological conditions with variable penetrance and onset. Rectal prolapse developed in t-PA^{-/-}:u-PA^{-/-} mice at a significantly higher incidence than in u-PA^{-/-} mice (22 of 59 mice; 37%, $P < 0.001$ versus u-PA^{-/-} mice) and at an earlier age (12 ± 0.8 weeks; $P < 0.001$). As observed in u-PA^{-/-} mice, a small percentage of t-PA^{-/-}:u-PA^{-/-} mice (3 of 59 of 24 ± 1 weeks; 5%) had extensive non-healing ulcerations. A significant number of t-PA^{-/-}:u-PA^{-/-} mice (10 of 59; 17%) became runted, cachectic, dyspneic and died at 17 ± 2 weeks of age (the microscopical analysis of 6 of those is presented below). Such severe illness and early death was not observed in wild-type mice nor in mice with single inactivation of the t-PA or u-PA genes.

No histological abnormalities could be documented in any of the t-PA^{-/-} mice. u-PA^{-/-} mice displayed occasional occurrence of small, focal fibrin deposits in the intestines and in the sinusoids

FIG. 3 Light microscopic analysis of liver, colon, uterus and lung of preterminal $t\text{-PA}^{-/-}$: $u\text{-PA}^{-/-}$ mice (3 males of 8 to 15 weeks; 3 females of 12 to 23 weeks). **a**, Liver section revealing amorphous fibrin deposition (arrow) under the liver capsula (observed in all mice; haematoxylin–eosin staining; magnification, $\times 195$). Calcification (asterisk) of the fibrin deposits was frequently observed. **b**, Adjacent liver section stained according to von Kossa revealing black calcified lesions throughout the subcapsular liver parenchyma (magnification, $\times 79$). **c**, Immunostaining of a liver section with a murine fibrinogen/fibrin-specific antiserum (magnification, $\times 79$), revealing fibrin deposit. Specificity of the immunohistochemical staining was confirmed by preadsorption of the antiserum with murine fibrinogen which abolished positive staining, by the absence of similar fibrin-immunoreactive deposits in liver sections of wild-type mice and by the lack of staining with irrelevant primary antisera (data not shown). **d, e**, Colon sections stained with haematoxylin–eosin, revealing a superficial epithelial ulceration covered with fibrin (arrows in **d**; magnification, $\times 79$) and a subepithelial fibrin deposition (arrow in **e**; magnification, $\times 195$) (observed in 4 of 5 preterminal $t\text{-PA}^{-/-}$: $u\text{-PA}^{-/-}$ mice). **f**, Uterine section stained with haematoxylin–eosin revealing a large, subepithelial fibrin deposition (arrow) which extends in the stroma (asterisk) of the uterus (observed in 2 of 3 examined $t\text{-PA}^{-/-}$: $u\text{-PA}^{-/-}$ female mice; magnification, $\times 195$). **g**, Lung section stained with haematoxylin–eosin, revealing a triangular collapsed region of lung parenchyma, containing abundant fibrin deposition, which stained specifically with the murine fibrinogen/fibrin-specific antiserum (data not shown) (observed in 5 of 6 examined $t\text{-PA}^{-/-}$: $u\text{-PA}^{-/-}$ preterminal mice; magnification, $\times 79$).

METHODS. Preparation, fixation and staining of the tissues was as previously described³⁷. For immunohistochemistry, 5- μm sections from snap frozen liver and lung tissue were stained with a three-step indirect immunoperoxidase-method using primary goat anti-mouse fibrinogen/fibrin antibody, followed by peroxidase-conjugated rabbit anti-goat, and swine anti-rabbit immunoglobulins as second and third layers, respectively. Each incubation was at room temperature and followed by a 15-min wash in three changes of PBS, pH 7.2. The reaction product was developed by incubation for 15 min in 0.05 M acetate buffer (pH 4.9) containing



0.05% 3-amino-9-ethylcarbazole and 0.01% H_2O_2 , resulting in a red staining of immunoreactive sites. The sections were briefly counterstained with Harris' haematoxylin, and mounted with glycerin jelly.

of the liver and excessive fibrin deposits in the ulcerated skin, ear or prolapsed rectum (not shown). Histological abnormalities were only documented in $t\text{-PA}^{-/-}$: $u\text{-PA}^{-/-}$ mice beyond 2 to 3 months of age, with variable onset and penetrance and most prominently in preterminal $t\text{-PA}^{-/-}$: $u\text{-PA}^{-/-}$ mice. Preterminal $t\text{-PA}^{-/-}$: $u\text{-PA}^{-/-}$ mice revealed spontaneous fibrin deposits in liver, intestines, gonads, lungs (Fig. 3), in non-healing ulcerative lesions of the skin, ears and prolapsed rectum and occasionally in the kidneys (not shown). The fibrinous nature of the deposits was confirmed by immunostaining of frozen sections with a goat fibrinogen/fibrin-specific antiserum (Fig. 3c) and by electron-microscope analysis, which revealed the typical fibrillar structure and periodicity of fibrin polymers (not shown). Intestinal adhesions and occasionally ischaemic tissue necrosis (uterus and intestines), possibly resulting from thrombosis, were observed (not shown). The incidence of fibrin deposition in liver, intestines, gonads and lung was significantly higher in $t\text{-PA}^{-/-}$: $u\text{-PA}^{-/-}$ mice than in mice with any of the other genotypes studied

($P < 0.001$ to $P < 0.05$) (see supplementary information).

Thrombolysis and thrombosis

The role of $t\text{-PA}$ and $u\text{-PA}$ in spontaneous clot lysis was evaluated by determining the *ex vivo* lysis of ^{125}I -fibrin-labelled plasma clots, which were injected through the jugular vein and embolized into the pulmonary arteries²⁵. No difference in the rate of spontaneous plasma clot lysis was observed between the wild-type and $u\text{-PA}^{-/-}$ mice ($85 \pm 4\%$ versus $83 \pm 9\%$ lysis over 24 h, respectively; P not significant) (Fig. 4). In contrast, $t\text{-PA}^{-/-}$ mice lysed pulmonary plasma clots at a significantly reduced rate ($21 \pm 3\%$ lysis over 24 h, $P < 0.001$ versus wild-type mice) but pulmonary clot lysis was most prominently reduced in the $t\text{-PA}^{-/-}$: $u\text{-PA}^{-/-}$ mice ($3 \pm 3\%$ lysis within 24 h in $t\text{-PA}^{-/-}$: $u\text{-PA}^{-/-}$ mice, $P < 0.002$ versus $t\text{-PA}^{-/-}$ mice). Pulmonary plasma clot lysis remained significantly lower in the combined $t\text{-PA}^{-/-}$: $u\text{-PA}^{-/-}$ mice than in the $t\text{-PA}^{-/-}$ mice for up to 48 h, but was not significantly different after 72 h (Fig. 4).

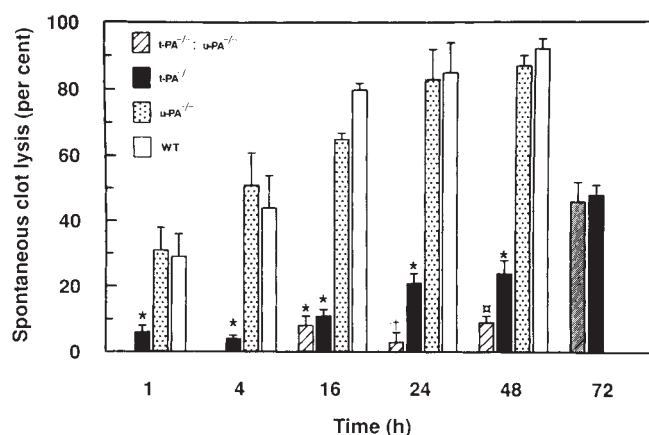


FIG. 4 Spontaneous lysis of a ^{125}I -fibrin-labelled pulmonary plasma clot. A $25\ \mu\text{l}$ ^{125}I -fibrin-labelled plasma clot was injected into the jugular vein and the residual radioactivity in heart and lungs measured *ex vivo* at the indicated time points. Values are expressed as a per cent of total radioactivity injected. $t\text{-PA}^{-/-}$ mice lysed ^{125}I -fibrin-labelled plasma clots more slowly than $u\text{-PA}^{-/-}$ or wild-type mice; lysis of the plasma clots was slowest in $t\text{-PA}^{-/-}; u\text{-PA}^{-/-}$ mice. *, $P < 0.001$ versus wild-type and versus $u\text{-PA}^{-/-}$ mice. †, $P < 0.002$, ††, $P = 0.01$ versus $t\text{-PA}^{-/-}$ mice. Preparation *in vitro* and lysis *in vivo* of ^{125}I -fibrin-labelled plasma clots in mice was as previously described.²⁵

$t\text{-PA}$ - and $u\text{-PA}$ -deficient mice were tested for their susceptibility to venous thrombosis after local injection of proinflammatory endotoxin in the footpad, a model which is sensitive to alterations of the fibrinolytic system²⁶. Injection of 10 or 20 μg endotoxin (endotoxin W. from *Escherichia coli* 0111:B4 or from *Salmonella typhosa* 908) induced venous thrombosis in 29 of 54 wild-type mice (54%), in 29 out of 38 $t\text{-PA}$ -deficient mice (76%, $P = 0.046$ versus wild-type mice, by chi-square analysis) and in 27 out of 30 $u\text{-PA}$ -deficient mice (90%, $P = 0.002$ versus wild-type mice). The extent of venous thrombosis, as estimated from the number of veins with visible thrombi, was significantly higher in the $t\text{-PA}^{-/-}$ and $u\text{-PA}^{-/-}$ mice. Only 15% of the wild-type but 55% of the $t\text{-PA}^{-/-}$ mice ($P < 0.001$) and 60% of the $u\text{-PA}^{-/-}$ mice ($P < 0.001$) contained more than 4 thrombosed veins per analysed tissue section.

Macrophage function

To examine whether $u\text{-PA}$ might allow extracellular matrix degradation^{8,27}, lysis of ^{125}I -fibrin-labelled matrix and of ^3H -proline-labelled subendothelial matrix by thioglycollate-stimulated macrophages (which have a 10- to 100-fold enhanced production of $u\text{-PA}$ ⁸) was studied. Disruption of the $u\text{-PA}$ genes specifically abolished plasminogen-dependent breakdown of ^{125}I -fibrin-labelled matrix and of ^3H -proline-labelled subendothelial matrix breakdown by thioglycollate-activated macrophages (Fig. 5), but $u\text{-PA}$ deficiency did not affect invasion of macrophages into the peritoneal cavity after thioglycollate injection (Fig. 5). Matrix degradation by thioglycollate-activated macrophages was not affected by inactivation of the $t\text{-PA}$ genes (Fig. 5). These results indicate that $u\text{-PA}$ -mediated plasmin formation may aid in breakdown of fibrin deposits or matrix components, but that in the absence of $u\text{-PA}$, invasion by macrophages is unaltered under the present experimental conditions.

Discussion

The physiological plasminogen activators $t\text{-PA}$ and $u\text{-PA}$ share the characteristic ability to activate plasminogen, but have distinct protein structures, tissue-specific expression and biological activities, suggesting that these molecules may play distinct roles in different biological processes¹⁻³. Much circumstantial evidence

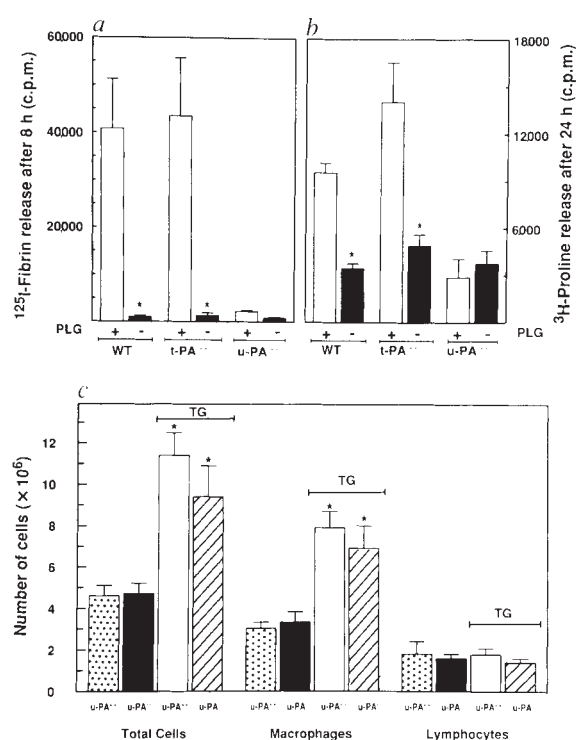


FIG. 5 Matrix degradation and invasion into the peritoneal cavity by thioglycollate-stimulated macrophages. a, b, Lysis of ^{125}I -fibrin matrix (a) and of ^3H -proline-labelled subendothelial matrix (b) by thioglycollate-stimulated macrophages from wild-type, $t\text{-PA}^{-/-}$ and $u\text{-PA}^{-/-}$ mice. PLG (+): with $16\ \mu\text{g}\ \text{ml}^{-1}$ plasminogen in the culture medium; PLG (-): without plasminogen; WT: wild-type. The data represent mean \pm s.e.m. of triplicate measurements of 5 or 6 independent experiments. $P < 0.05$ versus PLG (+). c, Invasion into the peritoneal cavity of thioglycollate-stimulated macrophages from $u\text{-PA}^{+/+}$ and $u\text{-PA}^{-/-}$ mice. Macrophages from $u\text{-PA}^{-/-}$ mice invaded the peritoneal cavity equally well as macrophages from $u\text{-PA}^{+/+}$ mice, both with or without thioglycollate injection. The data represent mean \pm s.e.m. of 6 experiments. Cell counts were done on at least 200 cells. TG, with intraperitoneal injection of 0.5 ml thioglycollate; *, $P < 0.05$ versus control. METHODS. Preparation and lysis of ^{125}I -fibrin and ^3H -proline subendothelial matrix by thioglycollate-stimulated peritoneal macrophages was as described¹⁰. Invasion was evaluated by injecting mice intraperitoneally with 0.5 ml thioglycollate and counting, after 3 days, the number of different cell types in the peritoneal lavage⁹.

implicates these plasminogen activators in ovulation^{11,12}, sperm migration and fertilization¹⁶, embryo implantation^{17,20}, embryogenesis^{18,19} and associated tissue remodelling of the ovary^{17,28}, prostate, and mammary gland^{29,30}, but no genetic deficiencies involving either gene product have been described in man. Thus, inactivation of $t\text{-PA}$ or $u\text{-PA}$ genes in mice might have been anticipated to result in a lethal phenotype. Surprisingly, single- and double-deficient mice appear normal at birth, suggesting that neither $t\text{-PA}$ nor $u\text{-PA}$, individually or in combination, is required for normal embryonic development. Although doubly deficient mice are able to reproduce, they are significantly less fertile than wild-type mice or mice with a single deficiency of $t\text{-PA}$ or $u\text{-PA}$, possibly because of the poor general health of these animals (low body weight, dyspnoea, rectal prolapse and cachexia) or to the large fibrin deposits in their gonads. These data suggest that proteinases³¹ other than $t\text{-PA}$ and $u\text{-PA}$ may be more essential in reproduction and embryonic development than previously suspected.

These targeting experiments reveal a divergent and specific role for each plasminogen activator in fibrinolysis and macrophage function. The role of $t\text{-PA}$ and $u\text{-PA}$ in the normal surv-

TABLE 1 t-PA and u-PA activity in wild-type and homozygous t-PA-deficient (t-PA^{-/-}) or u-PA-deficient (u-PA^{-/-}) mice

Mice	t-PA activity		u-PA activity	
	Lung (IU mg ⁻¹)	Brain (IU mg ⁻¹)	Kidney (IU mg ⁻¹)	Urine (IU)
t-PA ^{+/+}	5.0 ± 0.8 (5)	5.6 ± 0.4 (5)	ND	99 ± 35 (8)
t-PA ^{+/-}	1.7 ± 0.3* (5)	ND	ND	ND
t-PA ^{-/-}	<0.1 (5)	<0.3 (5)	ND	120 ± 23 (9)
u-PA ^{+/+}	ND	5.6 ± 0.8 (5)	0.46 ± 0.1 (5)	131 ± 19 (9)
u-PA ^{+/-}	ND	ND	0.22 ± 0.02* (5)	ND
u-PA ^{-/-}	ND	5.7 ± 1.3 (3)	<0.05 (5)	<3.1

Values represent mean ± s.e.m. of activities from the number of animals indicated in brackets. t-PA and u-PA activities are expressed as IU of murine t-PA or murine u-PA per mg protein in the tissue extracts (lung, brain, kidney) or as total units in 24-h urine samples. t-PA and u-PA activities were determined by the fibrin plate method³² (lung and kidney) or by a chromogenic substrate assay³³ (brain and urine) in the presence of 1 mM amiloride (which blocks murine u-PA) or of 200 µg ml⁻¹ murine t-PA-specific IgGs, respectively. The specific activity of murine u-PA, purified from endothelioma-conditioned medium¹³, was 26,000 IU mg⁻¹ and that of recombinant murine t-PA was 475,000 IU mg⁻¹, by comparison with the human standards, obtained from the National Institute for Biological Standards and Control (Hertford, UK). ND, not determined.

**P* < 0.05 versus wild-type mice. A direct correlation is observed between t-PA or u-PA activity in different tissues and the number of functional t-PA or u-PA alleles, respectively. No compensatory increase of t-PA or u-PA activity is observed in u-PA- or t-PA-deficient mice, respectively. t-PA or u-PA activities in tissue extracts from t-PA^{+/+} or u-PA^{+/+} mice, respectively, were not reduced by addition of tissue extracts from t-PA^{-/-} or u-PA^{-/-} mice, respectively (data not shown), indicating that absence of detectable t-PA or u-PA activity in tissue extracts from t-PA^{-/-} or u-PA^{-/-} mice, respectively, did not result from increased proteinase inhibitor activity.

ence of spontaneous fibrin deposition is supported by the observation that t-PA^{-/-} and t-PA^{-/-}:u-PA^{-/-} mice displayed a reduced or virtually absent endogenous lysis of ¹²⁵I-fibrin-labelled plasma clots, respectively, and the finding that u-PA-deficient and doubly deficient mice suffered occasional or extensive spontaneous fibrin deposition, respectively. In addition, in response to proinflammatory endotoxin injection *in vivo*, overt thrombosis was observed in both t-PA- and u-PA-deficient mice at a significantly increased incidence and to a larger extent than

in wild-type mice. Possibly, impaired fibrin dissolution by u-PA-deficient macrophages may constitute a mechanism for the increased occurrence of venous thrombosis after endotoxin injection and the abnormal fibrin deposition in liver, skin and intestine in u-PA^{-/-} and t-PA^{-/-}:u-PA^{-/-} mice. Collectively, these data confirm the role of the fibrinolytic system in maintaining vascular patency² and suggest that fibrinolysis may play a significant role in preventing thrombosis in conditions of inflammation and injury. Further examination of the effect of t-PA and u-PA gene disruption in pathological disorders such as atherosclerosis²², glomerulonephritis²³ and malignancy¹⁵ seems to be warranted.

One unresolved issue is whether the observed phenotype of spontaneous fibrin deposition in t-PA^{-/-}:u-PA^{-/-} mice occurs as a result of the markedly reduced thrombolytic potential or secondary to deficient tissue remodelling. u-PA has been proposed to modulate tissue remodelling through activation of matrix-degrading proteinases and growth factors^{6,7}. Finally, the apparently normal invasiveness of u-PA^{-/-} macrophages and trophoblasts (as revealed by the normal reproduction of u-PA^{-/-} mice) might suggest a less prominent role of u-PA in cellular invasion than previously suspected. Other processes of cellular invasion such as in tumorigenesis¹⁵ and endothelial or vascular smooth muscle cell migration^{3,6,7} still need to be examined further.

The phenotypes of mice with a single deficiency of t-PA or u-PA would appear to result, at least in part, from the ability of one plasminogen activator to complement the other. Mice with a combined deficiency of t-PA and u-PA present with spontaneous fibrin depositions at a significantly increased incidence, to a larger extent, and in more organs than observed in the single mutants, and suffer retarded postnatal growth and a markedly reduced fertility and life expectancy. The almost total lack of endogenous lysis of a ¹²⁵I-fibrin plasma clot and the higher incidence and earlier occurrence of the rectal prolapse in the doubly deficient mice further support the notion that u-PA and t-PA cooperate in a variety of biological phenomena, possibly related to fibrin degradation, matrix remodelling and/or growth factor activation^{6,7}.

This study indicates that the t-PA and u-PA gene products have divergent roles in fibrinolysis and macrophage function and that they cooperate in a number of complex biological processes. Although their combined deficiency results in increased morbidity and mortality, it does not appear to affect embryonic development. □

Received 19 November 1993; accepted 3 February 1994.

- Astrup, T. in *Progress in Chemical Fibrinolysis and Thrombolysis* Vol. 3 (eds Davidson, J.F., Rowan, R. M., Samama, M. M. & Desnoyers, P. C.) 1–57 (Raven, New York, 1987).
- Collen, D. & Lijnen, H. R. *Blood* **78**, 3114–3124 (1991).
- Vassalli, J. D., Sappino, A. P. & Belin, D. *J. clin. Invest.* **88**, 1067–1072 (1991).
- Kluft, C. *Tissue-type Plasminogen Activator (t-PA): Physiological and Clinical Aspects* Vol. 1 (ed. Kluft, C.) 47–79 (CRC, Boca Raton, Florida, 1988).
- Blasi, F., Vassalli, J.-D. & Dane, K. *J. Cell Biol.* **104**, 801–804 (1987).
- Saksela, O. & Rifkin, D. B. *A. Rev. Cell Biol.* **4**, 93–126 (1988).
- Moscattelli, D. & Rifkin, D. B. *Biochim. biophys. Acta* **948**, 67–85 (1988).
- Unkles, J. C., Gordon, S. & Reich, E. *J. exp. Med.* **139**, 834–850 (1974).
- Freyria, A. M., Paul, J., Belleville, J., Broyer, P. & Etoy, R. *Comp. Biochem. Physiol.* **99**, 517–524 (1991).
- Baker, M. S., Bleakley, P., Woodrow, G. C. & Doe, W. F. *Cancer Res.* **50**, 4676–4684 (1990).
- Huarte, J., Belin, D. & Vassalli, J. D. *Cell* **43**, 551–558 (1985).
- Tsafiri, A., Bicsak, T. A., Cajander, S. B., Ny, T. & Hsueh, A. J. W. *Endocrinology* **124**, 415–421 (1989).
- Wagner, E. F. *EMBO J.* **9**, 3024–3032 (1990).
- Morioka, S., Lazarus, G. S., Baird, J. L. & Jensen, P. J. *J. Invest. Dermatol.* **88**, 418–423 (1987).
- Dano, K. *et al. Adv. Cancer Res.* **44**, 139–266 (1985).
- Huarte, J., Belin, D., Bosco, D., Sappino, A. P. & Vassalli, J. D. *J. Cell Biol.* **104**, 1281–1289 (1987).
- Sappino, A. P., Huarte, J., Belin, D. & Vassalli, J. D. *J. Cell Biol.* **109**, 2471–2479 (1989).
- Strickland, S., Reich, E. & Sherman, M. I. *Cell* **9**, 231–240 (1976).
- Menoud, P. A., Debrot, S. & Schowing, J. *Roux Arch. dev. Biol.* **198**, 219–226 (1989).
- Denker, H. W. *Adv. Anat. Embryol. Cell Biol.* **53**, 3–123 (1977).
- Nilsson, I. M., Ljungner, H. & Tengborn, L. *Br. Med. J. Clin. Res. Ed.* **290**, 1453–1456 (1985).

- Juhan-Vague, I. & Collen, D. *Ann. Epidemiol.* **2**, 427–438 (1992).
- Tomooka, S., Border, W. A., Marshall, B. C. & Nobel, N. A. *Kidney Int.* **42**, 1462–1469 (1992).
- Idell, S. *et al. J. clin. Invest.* **84**, 695–705 (1989).
- Stassen, J. M., Vanlinthout, I., Lijnen, H. R. & Collen, D. *Fibrinolysis* **4** (suppl. 2) 15–21 (1990).
- Carmeliet, P. *et al. J. clin. Invest.* **92**, 2756–2760 (1993).
- Graneli-Piperno, A., Vassalli, J. D. & Reich, E. *J. exp. Med.* **146**, 1693–1706 (1977).
- Canipari, R., O'Connell, M. L., Meyer, G. & Strickland, S. *J. Cell Biol.* **105**, 977–981 (1987).
- Busso, N., Huarte, J., Vassalli, J. D., Sappino, A. P. & Belin, D. *J. Biol. Chem.* **264**, 7455–7457 (1989).
- Ossowski, L., Biegel, D. & Reich, E. *Cell* **16**, 929–940 (1979).
- Lala, P. K. & Graham, C. H. *Cancer Metastasis Rev.* **9**, 369–379 (1990).
- Astrup, T. & Müllertz, S. *Arch. Biochem. Biophys.* **40**, 346–351 (1952).
- Verheijen, J. H., Chang, G. T. G. & Kluft, C. *Thromb. Haemostasis* **51**, 392–395 (1984).
- Tybulewicz, V. L., Crawford, C. E., Jackson, P. K., Bronson, R. T. & Mulligan, R. C. *Cell* **65**, 1153–1163 (1991).
- Rickles, R. J., Darrow, A. L. & Strickland, S. *J. Biol. Chem.* **263**, 1563–1569 (1988).
- Peng, F., Ohlsson, M. & Ny, T. *J. Biol. Chem.* **265**, 2022–2027 (1990).
- Carmeliet, P. *et al. J. clin. Invest.* **92**, 2746–2755 (1993).
- Degen, S. J., Heckel, J. L., Reich, E. & Degen, J. L. *Biochemistry* **26**, 8270–8279 (1987).

ACKNOWLEDGEMENTS. We thank P. Holvoet and L. Nelles for cloning and expression of murine t-PA, and A. Bouché, C. Declercq, E. Demarsin, M. De Mol, S. Janssen, S. Pollefeyt, J. M. Stassen and S. Wynn for technical assistance. P.C. is a research associate of the NFWO. This work was supported by the NIH (R.C.M.) and the Belgian Instituut voor Wetenschap en Technologie and the Inter-Universitaire Attractiepolen (P.C., L.S., L.K., D.C.).

SUPPLEMENTARY INFORMATION. Requests should be addressed to Mary Sheehan at the London editorial office of *Nature*.